JOURNAL OF AIRCRAFT
Vol. 39, No. 3, May–June 2002

Unified Hypersonic/Supersonic Panel Method for Aeroelastic Applications to Arbitrary Bodies

P. C. Chen* and D. D. Liu†
ZONA Technology, Inc., Scottsdale, Arizona 85251-3540

A unified unsteady hypersonic/supersonic panel method has been developed and incorporated into ZAERO (a unified unsteady/steady aerodynamics/aeroelasticity methodology/software for aeroelastic applications). The present unified panel method is a viable design/analysis tool for future hypersonic flight vehicles and hypervelocity missiles. The method is established with a rotationality correction function to the general three-dimensional linear potential solution. An equivalent Mach number transformation is introduced to circumvent the superinclined panel limitation. Next, a local pulsating cone analogy is applied to each panel considered, thus yielding the in-phase and out-of-phase forces and moments for an arbitrary body with proper rotationality correction based on steady/unsteady Euler solutions. The obtained results were verified and validated with CFL3D solutions, AP98 results, and measured data. For all cases studied, the unified panel method is found to be computationally efficient (2–3 min per case), acceptably accurate, and very versatile in its applicability, including aerodynamic/stability derivative/aeroelastic/aeroservoelastic applications for complex wing–body or missile-fin configurations in the unified hypersonic/supersonic flight regime.

Nomenclature

A_B = body base area
C_M = pitch moment$/(1/2\rho U_\infty^2 A_B L)$
C_{M_q} = $\partial C_M/\partial(qL/U_\infty)$
C_{M_α} = $\partial C_M/\partial\alpha$
$C_{M_{\dot\alpha}}$ = $\partial C_M/\partial(\dot\alpha L/U_\infty)$
C_N = normal force$/(1/2\rho U_\infty^2 A_B)$
C_{N_q} = $\partial C_N/\partial(qL/U_\infty)$
C_{N_α} = $\partial C_N/\partial\alpha$
$C_{N_{\dot\alpha}}$ = $\partial C_N/\partial(\dot\alpha L/U_\infty)$
L = reference length (body length)
P = pressure
q = angular velocity
S = body surface
U_∞ = freestream velocity α, angle of attack
γ = ratio of specific heats
ρ = density
σ = half-cone angle
ϕ = velocity potential
ω = harmonic frequency

I. Introduction

ALTHOUGH current computational fluid dynamics (CFD) methods have reached a rather mature stage for steady aerodynamic analysis, their design features may be hampered by the problem in grid generation and long computing time. A Navier–Stokes (N–S) code such as GASP[1] or CFL3D[2] for design/analysis of a missile body could consume over 24 h computing time for a simple flight condition. An N–S code could become even more inefficient, even if it were applied for unsteady two-dimensional aeroelastic applications, for example, in the case of an airfoil in limit-cycle oscillation. For this reason, more expedient methods, other than those of CFD origin, are encouraged by the design engineers. These methods will be integrated in a multidisciplinary optimization environment and with reasonable turnaround computing time. These types of expedient methods are apparently needed in hypersonic vehicle design, including that of transatmospheric vehicles and hypervelocity missiles. The current trend in kinetic energy missile design requires munition penetration at hypersonic velocities on impact. For design consideration, hypersonic control and maneuver of slender missiles require an accurate yet efficient hypersonic aerodynamic methodology. It is because of this demand that the present unified unsteady/steady hypersonic/supersonic method for treatment of general bodies is developed.

Developing an expedient unified hypersonic/supersonic aerodynamic method for flexible and rigid bodies is a challenging endeavor. One approach is to generalize the wing–body supersonic unsteady aerodynamic panel method[3] to include the hypersonic flight regime in the ZAERO software system.[4] Also included in the software system is a well-developed unified unsteady hypersonic/supersonic lifting surface treatment.[5,6] Here, the present effort is to extend a similar, but much less obvious, approach to the treatment of arbitrary bodies. It is well known that the problem in an unsteady supersonic panel arises from the so-called superinclined panels. A superinclined panel (SIP), usually located around body apex, is one on which the body slope is greater than the local Mach wave angle (Fig. 1a); hence, it causes a breakdown in the linear supersonic formulation. The SIP thus disallows the further extension of the integral linear supersonic flow to a higher Mach number regime. Classical approaches by Van Dyke[7,8] and by Tobak and Wehrend,[9] among many others, all showed this limitation in their supersonic methods.

Another problem in the present hypersonic extension attempt amounts to developing a suitable formulation for incorporating the flow rotationality effect into a linear supersonic potential model for bodies such as that adopted in the previous unified hypersonic/supersonic lifting surface treatment.[5,6] The present approach adopts an equivalent Mach number transformation to circumvent the SIP limitation, thus extending the supersonic panel method to a unified supersonic/hypersonic Mach number range. A formal derivation will be presented to introduce the rotationality correction term accounting for the shock/vorticity effects arising from the hypersonic aerodynamics. Finally, a local pulsating cone analogy method is developed to account for the steady/unsteady rotationality correction, thus yielding the proper in-phase and out-of-phase forces and moments for arbitrary bodies.

Received 31 October 2000; revision received 4 September 2001; accepted for publication 24 September 2001.

*President, Department of Mechanical Aerospace Engineering; pc@zonatech.com. Member AIAA.
†Professor, Arizona State University, Aeroservoelastic; danny.liu@asu.edu. Associate Fellow AIAA.

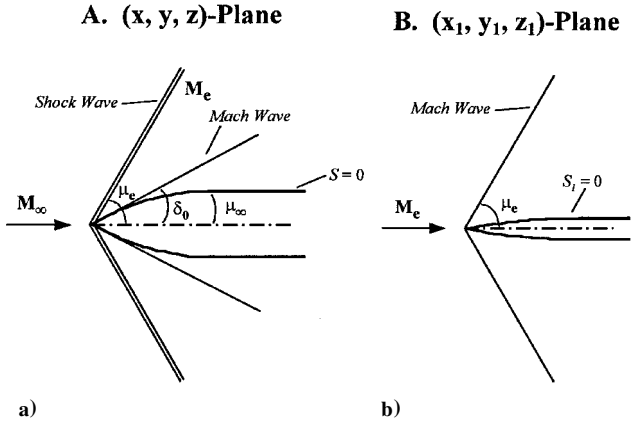

Fig. 1 Equivalent Mach number transformation: problem A to B.

II. Perturbed Euler Equations

Consider the time-dependent three-dimensional Euler equations, that is,

$$\frac{\partial \rho}{\partial t} + \nabla \cdot (\rho \boldsymbol{V}) = 0 \tag{1}$$

$$\frac{\mathrm{D}\boldsymbol{V}}{\mathrm{D}t} = -\frac{1}{\rho}\nabla P \tag{2}$$

$$\frac{\mathrm{D}}{\mathrm{D}t}(P\rho^{-\gamma}) = 0 \tag{3}$$

where the flow velocity reads

$$\boldsymbol{V} = u\boldsymbol{i} + v\boldsymbol{j} + w\boldsymbol{k}$$

the gradient vector reads

$$\nabla = \frac{\partial}{\partial x}\boldsymbol{i} + \frac{\partial}{\partial y}\boldsymbol{j} + \frac{\partial}{\partial z}\boldsymbol{k}$$

and the substantial derivative reads

$$\frac{\mathrm{D}}{\mathrm{D}t} = \frac{\partial}{\partial t} + \boldsymbol{V} \cdot \nabla$$

The general tangency condition (TC) requires that no normal velocity at the body surface at all times, that is,

$$\frac{\mathrm{D}S}{\mathrm{D}t} = 0 \qquad \text{at} \qquad S = z - f(x, y, t; \tau, \delta)$$

where τ is the body thickness and δ is the body oscillatory amplitude.

Consider a hyperbolic equation system with freestream Mach number being supersonic or hypersonic. The flow solution of the Euler equations (1–3), can be expressed in three terms, that is,

$$P = P_0 + P', \qquad \rho = R_0 + \rho', \qquad \boldsymbol{V} = (U_0 + u', v', w') \tag{4}$$

where P_0, R_0, and U_0 are the mean flow properties behind the shock and the prime properties are the perturbed pressure, density, and flow velocities due to unsteady amplitude motion.

If P_0, R_0, and U_0 are slowly variant or correspond to a stationary local flow (such as the flow behind a wedge or that of a constant density hypersonic flow), then the perturbed flow can be linearized, resulting in a single second-order accoustic equation in terms of pressure, that is,

$$\left(M_0^2 - 1\right)\frac{\partial^2 P'}{\partial x^2} - \frac{\partial^2 P'}{\partial y^2} - \frac{\partial^2 P'}{\partial z^2} + 2M_0^2\frac{\partial^2 P'}{\partial x\,\partial t} + M_0^2\frac{\partial^2 P'}{\partial t^2} = 0 \tag{5}$$

where M_0 represents the Mach number of the slowly variant flowfield behind the shock or that of the constant density flow. Clearly, in the case of linear potential flow, M_0 becomes the freestream Mach number M_∞ as the shock wave degenerates into the Mach wave. Thus, the linearized P' is the acceleration potential, a basis for panel method formulation, that is,

$$P' \approx \bar{\psi} \equiv \frac{\partial \phi}{\partial t} + U_\infty \frac{\partial \phi}{\partial x} \tag{6}$$

where ϕ is the unsteady perturbed potential.

Equation (5) is then reduced to the familiar unsteady potential equation or the acoustic equation in ϕ, that is,

$$\left(M_\infty^2 - 1\right)\phi_{xx} - \phi_{yy} - \phi_{zz} + 2M_\infty^2\phi_{xt} + M_0^2\phi_{tt} = 0 \tag{7}$$

III. Rotationality Correction Formulation

Let $\boldsymbol{x}$ denote the field point (x, y, z). Equation (4) can be explicitly expressed as

$$P(\boldsymbol{x}, t) = P_0(\boldsymbol{x}) + P'(\boldsymbol{x}, t)$$

It can be recast into a form of

$$P(\boldsymbol{x}, t) = \bar{\psi}(\boldsymbol{x}, t) + \Delta P(\boldsymbol{x}, t) \tag{8}$$

where $\Delta P = P_0 + P' - \bar{\psi}$ is a rotationality correction to the linearized acceleration potential of the linear potential solution.

The rotationality correction formulation of Eq. (8) suggests that the pressure coefficient can be expressed in two parts, that is,

$$C_P(\boldsymbol{x}, t) = \bar{C}_P(\boldsymbol{x}, t) + \Delta C_P(\boldsymbol{x}, t) \tag{9}$$

where $\bar{C}_P$ corresponds to the pressure coefficient derived from the potential methods such as that of ZONA7,[3,10] and ΔC_P is the rotationality correction pressure coefficient (RCP).

The formulation of Eq. (9) amounts to the classical splitting of the velocity field by many in the past (for example, Lighthill,[11] Sears,[12] and Carrier[13]), that is,

$$\boldsymbol{V} = \nabla\phi + \Delta\boldsymbol{V} \tag{10}$$

where ϕ is the velocity potential solution of the linear potential equation (7), as solved by ZONA7, and $\Delta\boldsymbol{V}$ is the rotationality correction term to the ϕ solution.

The present rotationality-correction approach is in line with a consistent approach that has been adopted in the transonic nonlinearity correction method[14] and in the hypersonic rotationality correction method for lifting surfaces.[5,6] This is to say that all of these nonlinear correction methods are applied to a based linear potential solution that is unsteady, is three-dimensional, and can be computed by a panel method.

Next, Eqs. (7) and (9) will be recasted in the frequency domain. Consider an elastic body of length L (for which the rigid mode is a special case) performing bending oscillation in supersonic flow of speed U_∞ at a circular frequency ω with a small amplitude ε. If the harmonic oscillation is assumed, the velocity and potential can be expressed as

$$\boldsymbol{V} = \boldsymbol{v}e^{ikt}, \qquad \phi = \varphi e^{ikt}$$

Equations (7) and (9) can now be expressed as

$$\beta_\infty^2\varphi_{xx} - \varphi_{yy} - \varphi_{zz} + 2ikM_\infty^2\varphi_x - k^2M_\infty^2\varphi = 0 \tag{11}$$

where $\beta_\infty^2 = M_\infty^2 - 1$ and $k = \omega L/U_\infty$ is the reduced frequency.

The pressure correction Eq. (9) now becomes

$$C_P(\boldsymbol{x}; ik) = \bar{C}_P(\boldsymbol{x}; ik) + \Delta C_P(\boldsymbol{x}; ik) \tag{12}$$

Solutions of Eq. (11) and $\bar{C}_P$ of Eq. (12) can be obtained by applying ZONA7, a supersonic panel method for wing–body and complex aircraft/missile configurations.[3]

IV. Equivalent Mach Number Transformation

As discussed, the applicability of the linear integral methods for solving Eq. (11) is confined by the limitation of SIP. An SIP Mach number is defined by a freestream Mach number whose Mach wave angle, $\mu_\infty = \sin^{-1}(1/M_\infty)$, is equal to the local body (or panel) slope. Almost all classical supersonic integral methods based on Eq. (11) cease to be valid beyond the SIP Mach number limit, for example, those of Van Dyke[7,8] and Tobak and Wehrend.[9] The outstanding work by Kacprzynski and Landahl[15] has shown a modified supersonic integral solution method can be extended beyond such an SIP Mach number limit, if one adopts the local linearization strategy for the supersonic kernels. However, the method itself does not formally include rotationality, let alone the Newtonian limit. A supersonic, not-so-slender body solution (for example, that of Adams and Sears[16]), on the other hand, is not confined by the SIP limit, but only lends itself to the near-field solutions for bodies of revolution. Neither method, in fact, has the potential of extending to three-dimensional body treatments.

To circumvent the SIP limit, one introduces an equivalent Mach number transformation to recast the physical problem (problem A, Fig. 1b) into a new coordinate, whereby the body undergoes a compressibility stretch in the axial direction (problem B, Fig. 1b). This transformation reads

$$(x_1, y_1, z_1) = (\lambda x, y, z) \tag{13}$$

where $\lambda = \beta_e/\beta_\infty$, $\beta_e^2 = M_e^2 - 1$, and M_e is a selected equivalent supersonic Mach number of the problem.

The selection of M_e can be rather arbitrary, except that the equivalent Mach wave angle $\mu_e = \sin^{-1}(1/M_e)$ must be greater than the inclined angle of the panel, for example, δ_0 for the apex semicone angle of a pointed body (see Fig. 1a).

Consider a pointed body $S(x, y, z, t) = 0$ (see Fig. 1a). It appears that the aft-shock Mach number of the conical apex would be the best choice for M_e because it is the least possible Mach number to cause an SIP breakdown. Applying Eq. (13) to Eq. (11) yields the transformed equation (problem B),

$$-\beta_e^2\varphi_{x_1x_1} + \varphi_{y_1y_1} + \varphi_{z_1z_1} - 2ikM_\infty^2\lambda\varphi_{x_1} - k^2M_\infty^2\varphi = 0 \tag{14}$$

Meanwhile, the body surface is transformed into a slightly stretched one (Fig. 1b), that is,

$$S(x, y, z, t) = 0 \rightarrow S_1(x_1, y_1, z_1, t) = 0 \tag{15}$$

whereas the freestream Mach number is replaced by M_e. Physically, the transformed problem becomes one with an equivalent freestream Mach number whose Mach wave is an exact degeneration of the corresponding shock wave of the given problem.

Furthermore, Eqs. (11) and (14) can be transformed to a universal linear supersonic equation, with the following transformations, respectively,

$$(x, y, z) = (\beta_\infty\xi, \eta, \zeta) \tag{15a}$$

$$(x_1, y_1, z_1) = (\beta_e\xi, \eta, \zeta) \tag{15b}$$

whereas the transformed equation becomes one with a freestream Mach number $M = \sqrt{2}$ and Mach wave of $\mu_1 = \pi/4$, that is,

$$-\varphi_{\xi\xi} + \varphi_{\eta\eta} + \varphi_{\zeta\zeta} - 2ik\left(M_\infty^2/\beta_\infty\right)\varphi_\xi - k^2M_\infty^2\varphi = 0 \tag{16}$$

This equation yields an oscillating potential corresponding to the harmonic gradient method for an unsteady supersonic lifting surface[17] as

$$\varphi = -\frac{1}{2\pi}\frac{\partial}{\partial n}\int\!\!\int_A \Delta\varphi(\xi_0, \eta_0, \zeta_0)H(\bar\xi, \bar\eta, \bar\zeta)\,\mathrm{d}\xi\,\mathrm{d}\eta \tag{17}$$

where

$$H(\bar\xi, \bar\eta, \bar\zeta) = [\cos(\upsilon R)/R]\exp(-i\upsilon M_\infty\bar\xi)$$

$$R = \sqrt{\bar\xi^2 - \bar\eta^2 - \bar\zeta^2}, \qquad \upsilon = kM_\infty/\beta_\infty$$

and $(\bar\xi, \bar\eta, \bar\zeta) = (\xi - \xi_0, \eta - \eta_0, \zeta - \zeta_0)$ is the hyperbolic field point-sending point distance.

Thus, the integral solution Eq. (17) can be solved by using ZONA7 subjected to the boundary condition (TC) applied at body $S_1 = 0$. The generalized TC, Eq. (4), applied at $S_1 = 0$ can be expressed as

$$A\nabla_1\varphi \cdot A\boldsymbol{n} = -\left\{ik\left(\frac{\boldsymbol{h}}{L}\right)\cdot A\boldsymbol{n} + \lambda\frac{\partial\boldsymbol{h}}{\partial x_1}\cdot A\boldsymbol{n}\right\} \tag{18}$$

where A is an operator such that

$$A\nabla_1 = \lambda\frac{\partial}{\partial x_1}\boldsymbol{i} + \frac{\partial}{\partial y_1}\boldsymbol{j} + \frac{\partial}{\partial z_1}\boldsymbol{k}, \qquad A\boldsymbol{n} = \lambda n_1\boldsymbol{i} + n_2\boldsymbol{j} + n_3\boldsymbol{k} \tag{19}$$

where $\boldsymbol{h}$ is the displacement vector of the flexible body and $\boldsymbol{n}$ is the direction normal of S_1.

The resulting solution in the (x_1, y_1, z_1) coordinate yields the velocities through the velocity influence coefficient matrix, for problem B, that is, $\boldsymbol{V}_1 = (u_1, v_1, w_1)$.

Because the TC of problem A is a special case of Eq. (18) by setting $\lambda = 1.0$, the velocities $\boldsymbol{V}_1$ can be related to $\boldsymbol{V}$ of problem A simply by the transformation in Eq. (13), that is,

$$(u, v, w) = (\lambda u_1, v_1, w_1) \tag{20}$$

Although the equivalent Mach number transformation formulation is formally derived, its selection of M_e is, nevertheless, an approximation. Therefore, solution discrepancy is expected from the present method. However, the discrepancy is slight because it can be shown that the error between $\boldsymbol{V}_1$ and $\boldsymbol{V}$ of the exact problem A only amounts to order of ε^4 ℓn ε and ε^4, where ε is the body thickness ratio.

V. Local Pulsating Cone Analogy

Because the mean flow is hypersonic/supersonic, the time required for it to travel a unit reference length L, for example, body length, is much faster than that required for one cycle of body oscillation. Thus, the corresponding unsteady problem can be treated as mildly unsteady in that flow history is only accounted for in the neighborhood of each panel. Hence, the rotationality effect (Sec. III) can be corrected locally as well. This suggests that the correction terms ΔC_P and $\Delta\boldsymbol{V}$ of Eqs. (9) and (10), when treated in the aerodynamic influence (AIC) or velocity inference coefficient matrices, can be modeled in a self-influenced manner. In other words, the incremented rotationality correction in terms of ΔC_P and $\Delta\boldsymbol{V}$ only appears along the diagonal of the AIC matrices, where the panel-to-panel influence is ignored. For each diagonal terms in the AIC matrix, the correction term ΔC_P can be expressed as

$$\Delta C_{P_R} = \left(\frac{\mathrm{d}C_{P_R}}{\mathrm{d}\delta}\right)_\sigma \cos\theta, \qquad \Delta C_{P_I} = \left(\frac{\mathrm{d}C_{P_I}}{\mathrm{d}\delta}\right)_\sigma \bar x\cos\theta \tag{21}$$

where θ is the azimuthal angle, σ is the semi-angle of the local cone (Fig. 2), $\bar x$ is the axial distance between the panel and the local cone apex (Fig. 2), and $(\mathrm{d}C_{P_R}/\mathrm{d}\delta)_\sigma$ and $(\mathrm{d}C_{P_I}/\mathrm{d}\delta)_\sigma$ are, respectively, the in-phase and out-of-phase pressure coefficients of the local cone undergoing a unit pulsating motion.

In fact, they can be related by the normal force derivatives in pitch, that is,

$$\Delta C_{N_\alpha} = \frac{1}{\pi\tan^2\sigma}\int_0^1\!\!\int_0^{2\pi}\left(\frac{\mathrm{d}C_{P_R}}{\mathrm{d}\delta}\right)_\sigma r(\cos^2\theta)\,\mathrm{d}\theta\,\mathrm{d}\bar x$$

$$= \frac{1}{2\tan\sigma}\left(\frac{\mathrm{d}C_{P_R}}{\mathrm{d}\delta}\right)_\sigma$$

$$\Delta C_{N_q} = \frac{1}{\pi\tan^2\sigma}\int_0^1\!\!\int_0^{2\pi}\left(\frac{\mathrm{d}C_{P_I}}{\mathrm{d}\delta}\right)_\sigma \bar x r(\cos^2\theta)\,\mathrm{d}\theta\,\mathrm{d}\bar x$$

$$= \frac{1}{3\tan\sigma}\left(\frac{\mathrm{d}C_{P_I}}{\mathrm{d}\delta}\right)_\sigma \tag{22}$$

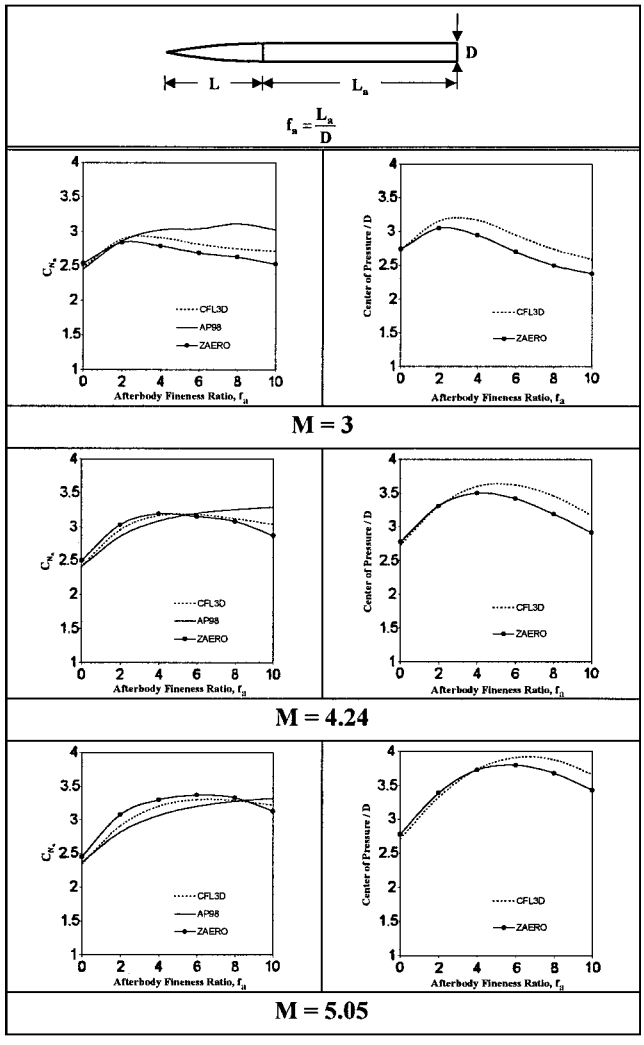

Fig. 2 Local pulsating cone analogy showing rotations.

where ΔC_{N_α} and ΔC_{N_q} are, respectively, the incremental stiffness and pitch-damping derivatives of the local cone. They are incremental in the sense that they represent the difference between the derivatives evaluated by the Euler computation vs that by the linear potential. They are, in fact, the rotationality correction components attributing to the ΔC_P correction. Explicitly, they are defined as

$$\Delta C_{N_\alpha} = C_{N_\alpha \text{Euler}}(M_\infty) - C_{N_\alpha \text{Potential}}(M_e)$$

$$\Delta C_{N_q} = C_{N_q \text{Euler}}(M_\infty) - C_{N_\alpha \text{Potential}}(M_e) \qquad (23)$$

The exact Euler values of C_{N_α} and C_{N_q} for an oscillating cone were given by Sims[18] and Brong,[19] whereas the exact potential values of the same were given by Tobak and Wehrend.[8]

VI. Results and Discussion

Several case studies are presented for various bodies using the present unified hypersonic/supersonic panel method (denoted by ZAERO throughout). These include: 1) pressure distribution of the bent-nose (ogive–cylinder) body, 2) the static stability derivatives of cones and ogive–cylinder bodies, and 3) the dynamic stability derivatives of cone, cone-frustum, and ogive–cylinder bodies. Computed results are presented to validate the present results with that of CFL3D using its Euler option.

A. C_P of the Bent-Nose Ogive–Cylinder Body

Provided by the U.S. Army Missile Command (MRDEC) as related in a private communication by L. Auman (May 2000) the bent-nose body is the centerbody of a compact kinetic energy missile (CKEM) design. Shown in Fig. 3, the bent-nose body has the slender ratio of $\tau = 0.0435$, but with a hypersonic parameter $k = 1.5$ ($M_\infty = 6.0$ and ogive apex angle $\theta = 14$ deg). Five flight conditions were computed, all at $M_\infty = 6.0$ (see Table 1).

For undeflected-nose cases (Figs. 3 and 4), the agreements in C_P are very good between the present unified panel method and CFL3D. Note that the kink in C_P is a typical inviscid result due to the slope discontinuity at the ogive–cylinder juncture.

Table 1 Five bent-nose body configurations

Figures	Body α, deg	Nose α, deg	Ogive nose deflection (bent nose)
3	0	0	No
4	−2	−2	No
5	−2	0	Yes
6	0	2	Yes
7	2	4	Yes

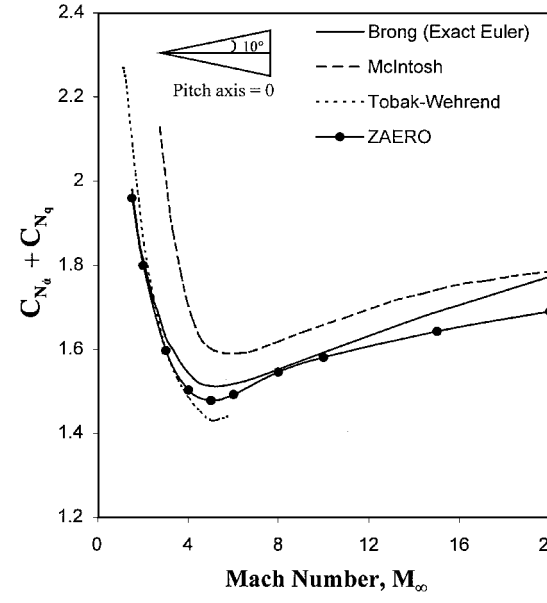

Fig. 3 Positive 2-deg deflection between nose and body (0-deg body, 0-deg nose, and $M = 6$).

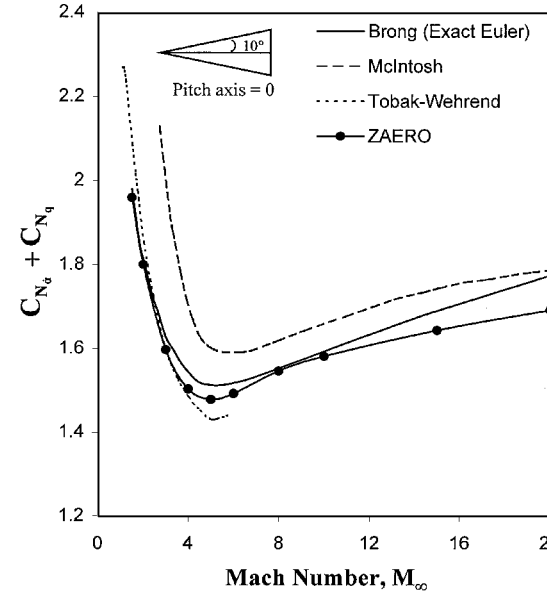

Fig. 4 Undeflected case, body, and nose at same angle of attack (− 2-deg body, − 2-deg nose, and $M = 6$).

Table 2 Comparison of bent-nose body lift, moment, drag and hinge moment ZAERO vs CFL3D[a]

CFL3D				Present panel method			
C_L[b]	C_M[c]	C_D[d]	C_h[e]	C_L	C_M	C_D	C_h
−0.076	−0.02552	0.0553	3.76e−7	−0.0712	−0.02776	0.049	0
0.0437	0.0292	0.0492	0.00612	0.0408	0.02806	0.0493	0.00668
0.1637	0.0857	0.0537	0.0123	0.1517	0.08388	0.057	0.0133
−0.118	−0.0549	0.0465	−0.00612	−0.1125	−0.05588	0.050	−0.00668

[a] $A_B = 2.405$ in.^{2}, $L = 40.25$ in.
[b] C_L = lift force/$q_\infty A_B$.
[c] C_M = pitch moment about c.g./$q_\infty A_B L$.
[d] C_D = drag force/$q_\infty A_B$.
[e] C_h = hinge moment of nose section about $x = 7$ in./$q_\infty A_B L$.

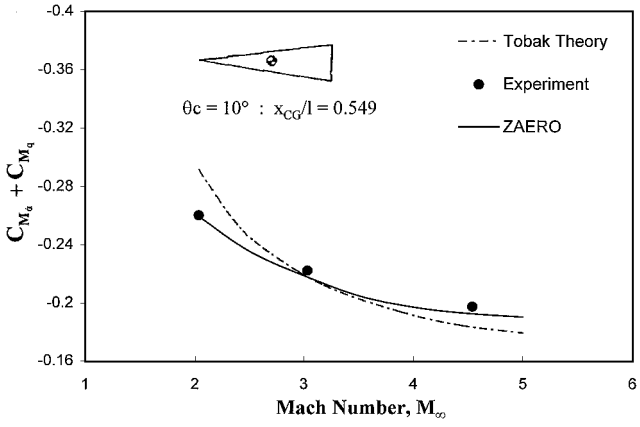

Fig. 5 Positive 2-deg deflection between nose and body (− 2-deg body, 0-deg nose, and $M = 6$).

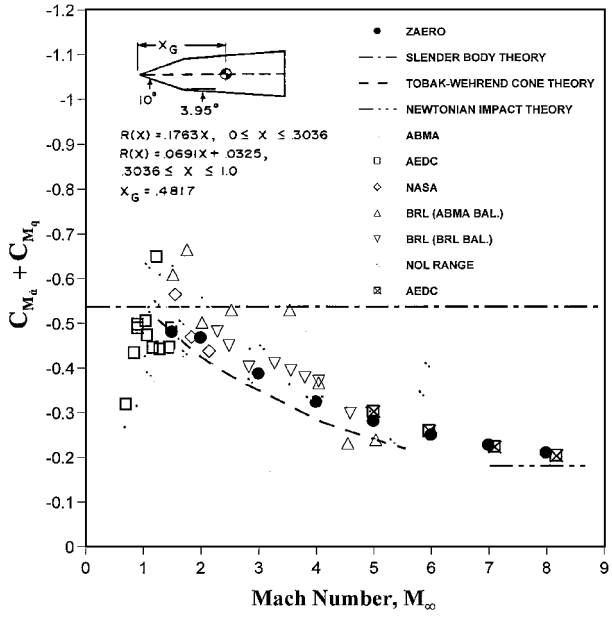

Fig. 6 Positive 2-deg deflection between nose and body (0-deg body, 2-deg nose, and $M = 6$).

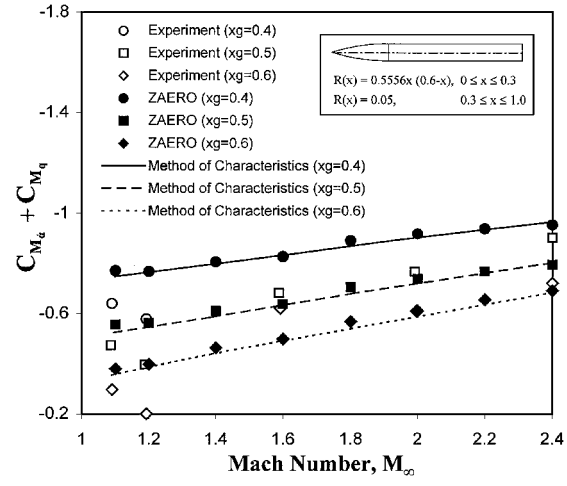

Fig. 7 Positive 2-deg deflection between nose and body (2-deg body, 4-deg nose, and $M = 6$).

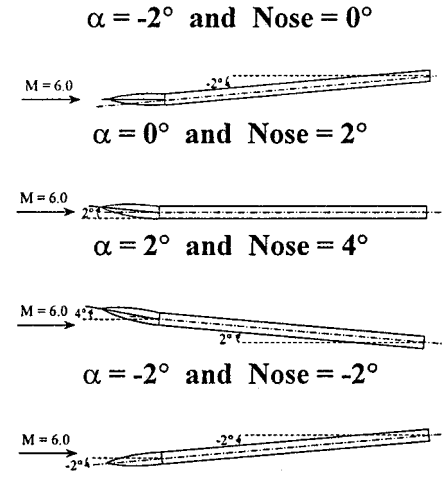

Fig. 8 Bent nose CKEM body at various angles of attack and bent nose angles.

For deflected-nose cases (Figs. 5–7), the overall C_P agreements are fair. Discrepancies at the ogive–cylinder juncture are seen as a result of the insufficiency in the present unified panel method, and CFL3D seems to occur at the expansion corner rather than the compression corner. This is expected because all compression panels are rotationality corrected, whereas the expansion panels only resume their linear potential values (rather than satisfying Euler), hence, overpredicting the expansion C_P. A further correction procedure can be developed using the method of characteristics scheme suggested by Ferri.[20] Finally, the coefficient of body normal force, moment, drag, and hinge moment (with respect to the ogive–cylinder junction at $x = 7$ in.) are summarized in Table 2 and diagramed in Fig. 8. For all cases considered, the discrepancies between the present results and CFL3D results range from 0 to 7%.

B. Static Stability Derivative: C_{N_α}

The normal force slopes with varying Mach numbers for 10- and 20-deg cones are presented, respectively, in Figs. 9 and 10. It is seen that the present results follow the same trend as Sim's exact (Euler) results,[18] but with acceptable discrepancy throughout the Mach number range from shock detachment to $M_\infty = 20$. The first- and second-order theory of Tobak and Wehrend[9] and Van Dyke[8] yield largely diverging results even in the moderate Mach number range. Their results were abruptly terminated at precisely the SIP Mach number, as explained earlier. Figure 11 compares C_{N_α} and center of pressure results of an ogive–cylinder body of an extendable

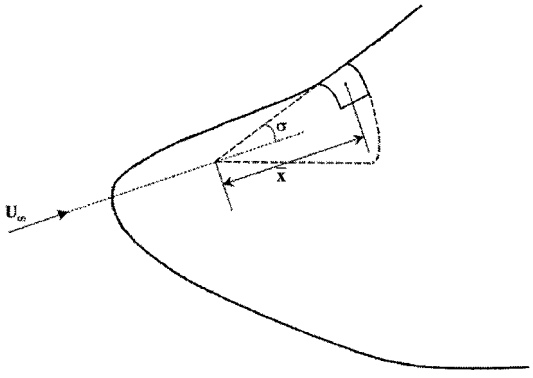

Fig. 9 Variation with Mach number of the stability derivative (at cone angle = 10 deg).

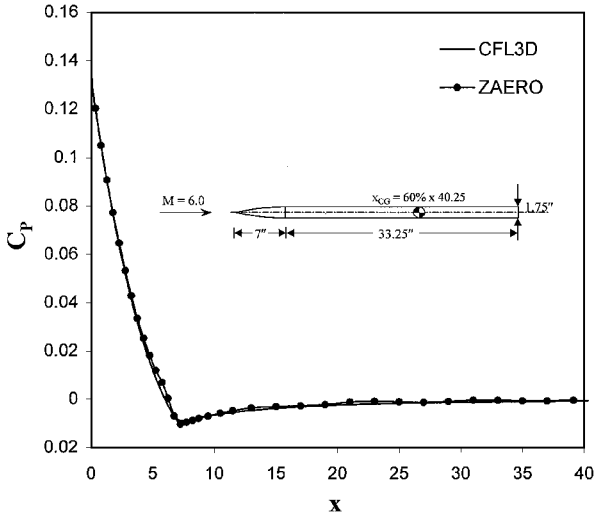

Fig. 10 Variation with Mach number of the stability derivative (at cone angle = 20 deg).

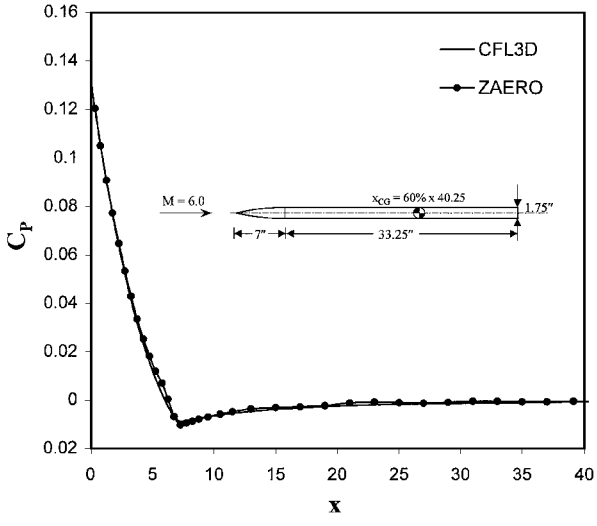

Fig. 11 $C_{N\alpha}$ and center of pressure of the ogive–cylinder body vs afterbody fineness ratio.

cylinder aft-body at $M_\infty = 3.0$, 4.24, and 5.05. Overall, the present results compare favorably with that of CFL3D. The AP89 (shock expansion method)[21] results tend to overpredict C_{N_α} values with increased afterbody fineness ratio.

C. Dynamic Stability Derivatives: $C_{N_{\dot\alpha}} + C_{N_q}$ and $C_{M_{\dot\alpha}} + C_{M_q}$

The coefficients of out-of-phase forces with varying Mach numbers for a pitching 10-deg cone and a 20-deg cone about the apex are presented, respectively, in Figs. 12 and 13. It is seen that the present

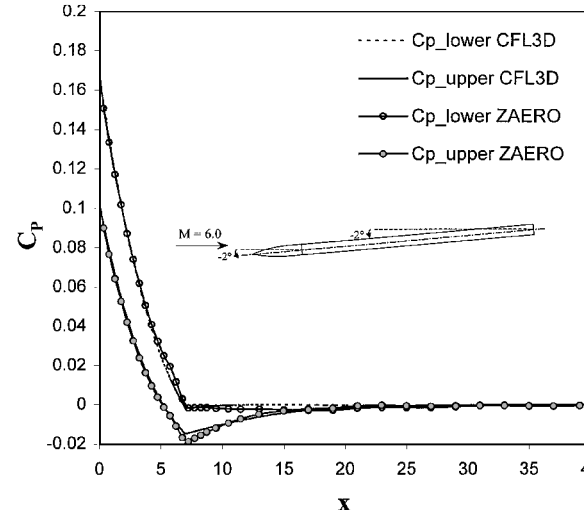

Fig. 12 Variation with Mach number of the stability derivative (at cone angle = 10 deg).

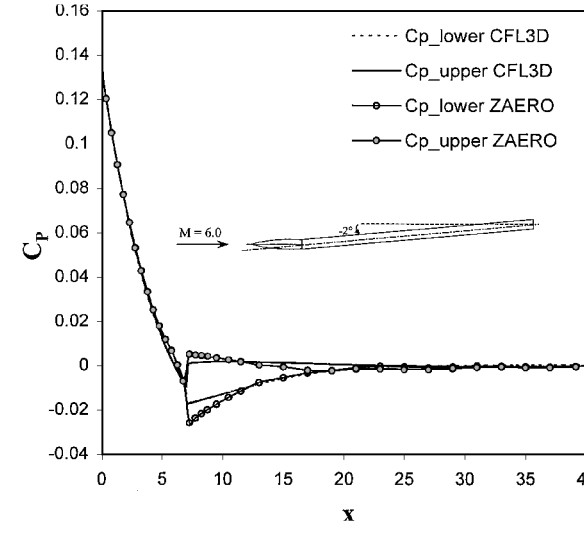

Fig. 13 Variation with Mach number of the stability derivative (at cone angle = 20 deg).

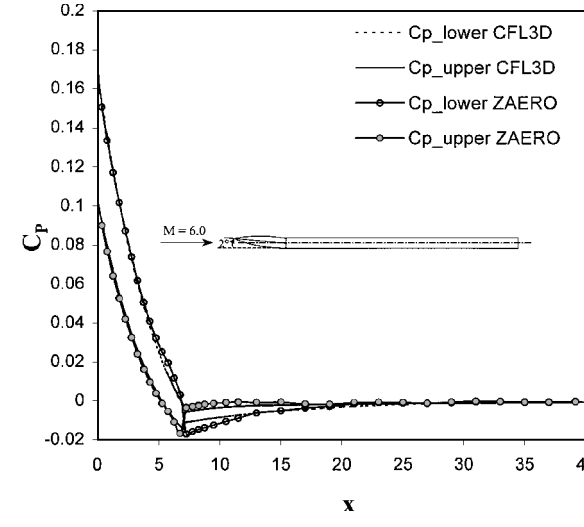

Fig. 14 Predicted and measured damping of a 10-deg sharp cone.

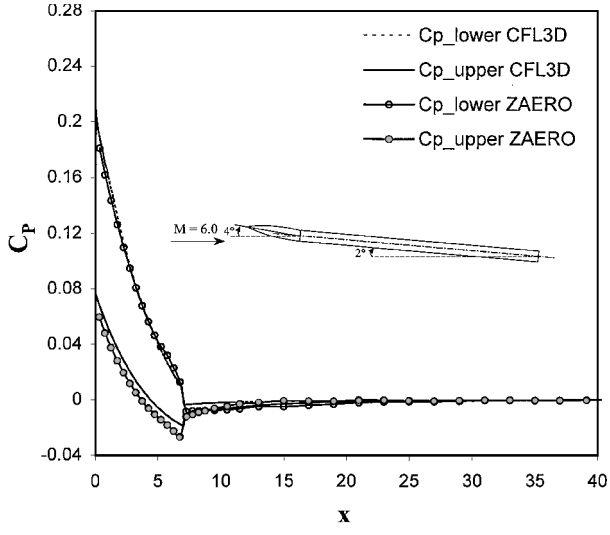

Fig. 15 Comparison of theoretical and experimental damping-in-pitch moment coefficients for a cone frustum at various Mach numbers.

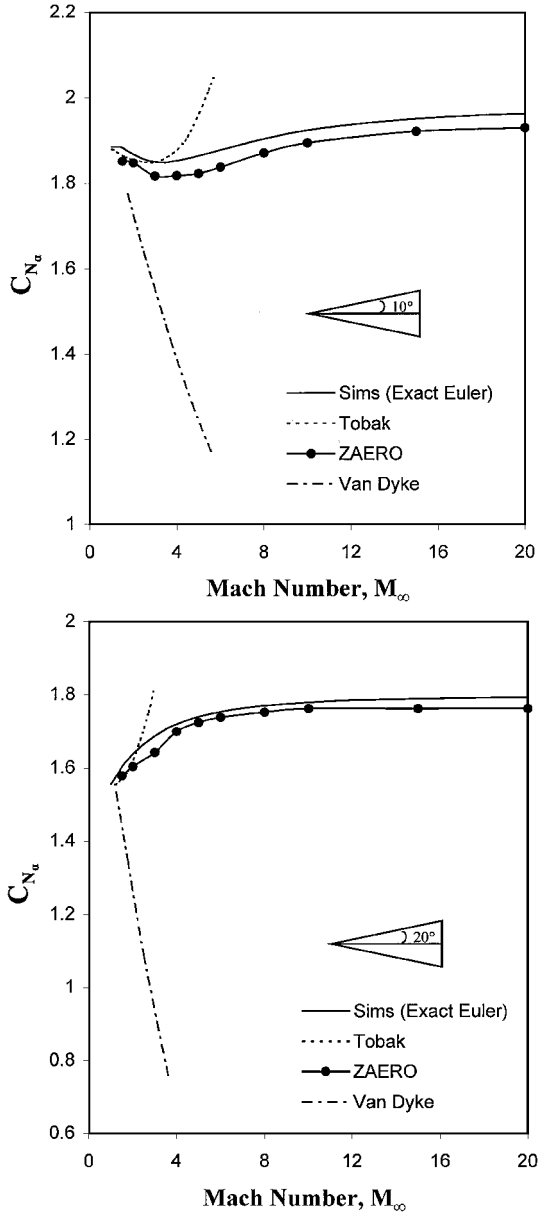

Fig. 16 Effect of Mach number on fixed axis damping in pitch moment coefficient for an ogive cylinder.

results largely follow the same trend as Brong's[19] exact Euler solutions, but again with acceptable discrepancy, throughout the Mach number range from shock detachment to $M_\infty = 20$. Much larger discrepancies were found between results of Tobak–Wehrend's[8] first-order theory and that of Brong's[19] exact Euler solution. McIntosh's numerical solution[22] agrees very well with Brong's[19] exact Euler solution at high Mach numbers, but large discrepancies are found at low to moderate supersonic Mach numbers. Figures 14–16 compare, respectively, the present pitch-damping results with measured data for an oscillating 10-deg cone–frustum and for a slender ogive–cylinder body at various range of moderate supersonic Mach numbers. Excellent agreements were found for all cases considered.

Conclusions

The following conclusions can be drawn from the present study:

1) A unified unsteady hypersonic/supersonic panel method has been developed and incorporated into the unified unsteady/steady aerodynamics/aeroelasticity methodology/software (ZAERO) for aeroelastic applications. Cases studied include the U.S. Army-provided bent-nose ogive–cylinder body, all at hypersonic/supersonic speeds. The results of the present unified hypersonic/supersonic panel method were verified and validated with other computational solutions (CFL3D and AP98) and measured data, respectively.

2) For a bent-nose body, close agreement in C_P, body normal force, moment, drag, and hinge moment with CFL3D solutions (within 0–7%) were found. Slight discrepancies in C_P were found at the lee side of the ogive–cylinder juncture with deflected nose. Improvement of the juncture aerodynamics for the expansion panels would await further incorporation of Ferri's[20] method-of-characteristics scheme.

3) The present unified hypersonic/supersonic panel method is found to yield excellent trends, following those of exact Euler steady/unsteady solutions, that is, those of Sims[18] and Brong,[19] in terms of static and dynamic stability derivatives, throughout all Mach numbers from shock detachment to Mach 20. Excellent agreements in pitch damping were established between the present results and measured data for various bodies. Expedient and accurate predictability in stability derivatives is one of superior features of the present panel method over existing methods.

4) The present unified hypersonic/supersonic panel method is shown to be very computationally efficient. For a typical bent-nose body case (see Figs. 3–7), a CFD code, such as CFL3D, would consume over 4 h of CPU time. By contrast, the developed method only requires 2–3 min on a 1-MB personal computer.

5) The current capability of the present unified steady/unsteady hypersonic/supersonic panel method can perform computations for aerodynamics/stability derivatives, aeroelastic, and ASE instability predictions at any speed for complex missile configurations. Given the capability, the high computation efficiency, and the acceptable efficiency of the present unified panel method, it should serve as a viable aerodynamic/aeroelastic tool for the design/analysis of future hypersonic flight vehicles, including transatmospheric vehicles and next-generation hypervelocity missiles.

Acknowledgments

The authors acknowledge the partial support of this research under a Dynetics/MRDEC contract. They wish to thank Lamar Auman of MREDC for initiation of this research topic and his providing the bent-nose body configuration and concept, thus allowing the validation of ZAERO vs CFL3D. The second author would like to acknowledge the full support by ZONA Technology, Inc. for funding of this work in its entirety.

References

[1] McGrory, W., Slack, D., Applebaum, M., and Walters, R., GASP Ver. 3.0, Aerosoft, Inc., Blacksburg, VA, 1996.

[2] Krist, S. L., Biedron, R. T., and Rumsey, C. L., "CFL3D User's Manual Version 5.0," NASA Langley Research Center, Sept. 1997.

[3]Chen, P. C., and Liu, D. D., "Unsteady Supersonic Computations of Arbitrary Wing-Body Configurations Including External Stores," *Journal of Aircraft*, Vol. 27, No. 2, 1990, pp. 108–116; also AIAA Paper 88-2309-CP, April 1988.

[4]Chen, P. C., and Sarhaddi, D., "ZAERO User's Manual Version 4.3," ZONA Technology, Inc., Scottsdale, AZ, June 2000.

[5]Liu, D. D., Yao, Z. X., Sarhaddi, D., and Chavez, F., "Piston Theory Revisited and Further Applications," *Journal of Aircraft*, Vol. 34, No. 3, 1997, pp. 304–312; also International Council of the Aeronautical Sciences, ICAS Paper 94-2.8.4, Sept. 1994.

[6]Liu, D. D., Chen, P. C., Yao, Z. X., and Sarhaddi, D., "Recent Advances in Lifting Surface Methods," *Aeronautical Journal of the Royal Aeronautical Society*, Vol. 100, No. 958, 1996, pp. 327–339.

[7]Van Dyke, M. J., "First-Order and Second-Order Theory of Supersonic Flow Past Bodies of Revolution," *Journal of Aeronautical Sciences*, Vol. 18, March 1951, pp. 161–178.

[8]Van Dyke, M. J., "Practical Calculation of Second-Order Supersonic Flow Past Non-Lifting Bodies of Revolution," NACA TN-2755, 1952.

[9]Tobak, M., and Wehrend, W. R., "Stability Derivatives of Cones at Supersonic Speeds," NACA TN-3788, Sept. 1956.

[10]Garcia-Fogeda, P., and Liu, D. D., "Analysis of Unsteady Aerodynamics for Elastic Bodies in Supersonic Flow," *Journal of Aircraft*, Vol. 24, No. 12, 1987, pp. 833–840; also AIAA Paper 86-0007, Jan. 1986.

[11]Lighthill, M. J., "The Diffraction of Blast," *Proceedings of the Royal Aeronautical Society of London*, A198, 1949, pp. 454–470.

[12]Sears, W. R., "Small Perturbation Theory," *General Theory of High Speed Aerodynamics and Jet Propulsion*, Vol. 6, Princeton Univ. Press, Princeton, NJ, 1954, Chap. C.

[13]Carrier, G. F., "The Oscillating Wedge in a Supersonic Stream," *Journal of the Aeronautical Sciences*, Vol. 16, No. 3, 1949, pp. 150–152.

[14]Chen, P. C., Sarhaddi, D., and Liu, D. D., "Transonic-Aerodynamic-Influence-Coefficient Approach for Aeroelastic and Multidisciplinary Optimization Application," *Journal of Aircraft*, Vol. 37, No. 1, 2000, pp. 85–94.

[15]Kacprzynski, J. J., and Landahl, M. T., "Recent Developments in the Supersonic Flow Over Axisymmetric Bodies with Continuous or Discontinuous Slope," AIAA Paper TP-67-5, Jan. 1967.

[16]Adams, M. C., and Sears, W. R., "Slender-Body Theory—Review and Extensions," *Journal of the Aerospace Sciences*, Vol. 20, 1953, pp. 85–98.

[17]Chen, P. C., and Liu, D. D., "A Harmonic Gradient Method for Unsteady Supersonic Flow Calculations," AIAA Paper 83-0887-CP, May 1983; also *Journal of Aircraft*, Vol. 22, No. 15, 1985, pp. 371–379.

[18]Sims, J. L., "Tables for Supersonic Flow Around Right Circular Cones at Small Angle of Attack," NASA SP-3007, 1964.

[19]Brong, E. A., "Flowfield about a Right Circular Cone in Unsteady Flight," AIAA Paper 65-398, July 1965.

[20]Ferri, A., "Supersonic Wave with Shock Waves," *General Theory of High Speed Aerodynamics and Jet Propulsion*, Vol. 6, Princeton Univ. Press, Princeton, NJ, 1954, Chap. H.

[21]Moore, F. G., McInville, R. M., and Hymer, T., "The 1998 Version of the NSWC Aero Prediction Code: Part 1—Summary of New Theoretical Methodology," U.S. Naval Surface Warfare Center, Dahlgren Div., Dahlgren, VA, NSWCDD/TR-98/1, April 1998.

[22]McIntosh, S. C., Jr., "The Studies in Unsteady Hypersonic Flow Theory," Ph.D. Dissertation, Dept. of Aeronautics and Astronautics, Stanford Univ., Stanford, CA, Aug. 1965.